BRAIN
A JOURNAL OF NEUROLOGY

Targeted loss of Arx results in a developmental epilepsy mouse model and recapitulates the human phenotype in heterozygous females

Eric Marsh,[1,2] Carl Fulp,[3] Ernest Gomez,[1,2] Ilya Nasrallah,[3] Jeremy Minarcik,[4] Jyotsna Sudi,[5] Susan L. Christian,[5] Grazia Mancini,[6] Patricia Labosky,[7] William Dobyns,[5,*] Amy Brooks-Kayal[8,*] and Jeffrey A. Golden[4]

1 Division of Neurology, Children's Hospital of Philadelphia, Department of Pediatrics, University of Pennsylvania, School of Medicine, Philadelphia, PA, USA
2 Department of Neurology, School of Medicine, University of Pennsylvania, Philadelphia, PA, USA.
3 Neuroscience Graduate Group, School of Medicine, University of Pennsylvania, Philadelphia, PA, USA
4 Department of Pathology, Children's Hospital of Philadelphia, School of Medicine, University of Pennsylvania, Philadelphia, PA, USA
5 Department of Human Genetics, Neurology and Pediatrics, University of Chicago, Chicago, IL, USA
6 Department of Clinical Genetics; Sophia Children's Hospital, Erasmus Medical Center, University of Rotterdam, Rotterdam, The Netherlands
7 Department of Cell and Developmental Biology, Vanderbilt University, Nashville, TN, USA
8 Department of Pediatrics, Division of Neurology, University of Colorado, Denver School of Medicine and The Children's Hospital, Aurora CO, USA

*These authors contributed equally to this work.

Correspondence to: Eric Marsh,
Abramson Research Center, Rm. 502,
Children's Hospital of Philadelphia,
3615 Civic Center Blvd.
Philadelphia, PA. 19104, USA
E-mail: marshe@email.chop.edu

Correspondence may also be addressed to: Jeffery A. Golden,
Department of Pathology,
Children's Hospital of Philadelphia,
School of Medicine,
University of Pennsylvania,
Philadelphia, PA, USA
E-mail: goldenj@mail.med.upenn.edu

Mutations in the X-linked aristaless-related homeobox gene (ARX) have been linked to structural brain anomalies as well as multiple neurocognitive deficits. The generation of Arx-deficient mice revealed several morphological anomalies, resembling those observed in patients and an interneuron migration defect but perinatal lethality precluded analyses of later phenotypes. Interestingly, many of the neurological phenotypes observed in patients with various ARX mutations can be attributed, in part, to interneuron dysfunction. To directly test this possibility, mice carrying a floxed Arx allele were generated and crossed to Dlx5/6^CRE-IRES-GFP(Dlx5/6^CIG) mice, conditionally deleting Arx from ganglionic eminence derived neurons including cortical interneurons. We now report that Arx^−/y;Dlx5/6^CIG (male) mice exhibit a variety of seizure types beginning in early-life, including seizures that behaviourally and electroencephalographically resembles infantile spasms, and show evolution through

development. Thus, this represents a new genetic model of a malignant form of paediatric epilepsy, with some characteristics resembling infantile spasms, caused by mutations in a known infantile spasms gene. Unexpectedly, approximately half of the female mice carrying a single mutant *Arx* allele ($Arx^{-/+};Dlx5/6^{CIG}$) also developed seizures. We also found that a subset of human female carriers have seizures and neurocognitive deficits. In summary, we have identified a previously unrecognized patient population with neurological deficits attributed to ARX mutations that are recapitulated in our mouse model. Furthermore, we show that perturbation of interneuron subpopulations is an important mechanism underling the pathogenesis of developmental epilepsy in both hemizygous males and carrier females. Given the frequency of *ARX* mutations in patients with infantile spasms and related disorders, our data unveil a new model for further understanding the pathogenesis of these disorders.

Introduction

The early epileptic encephalopathies are a group of malignant seizure syndromes with onsets in infancy or early childhood and a poor developmental prognosis. The most common malignant epilepsy is the infantile spasm syndrome (ISS or West syndrome) that is characterized by clusters of sudden flexion or extension of the trunk and limbs. They typically occur in clusters, have a specific EEG finding of hypsarrhythmia, and a poor developmental outcome (Zupanc, 2003). Various aetiologies can lead to the infantile spasm syndrome phenotype, including hypoxic ischaemic damage, malformations of cortical development and many genetic or developmental disorders such as Down syndrome and tuberous sclerosis (Zupanc, 2003). While activation of CNS corticotrophin releasing hormone (Brunson *et al.*, 2001) and interruption of the normal thalamo-cortical pathways (Frost and Hrachovy, 2005) have been proposed as mechanisms leading to the phenotypic convergence of the various etiologies, the pathogenesis and pathophysiology remain essentially unknown.

The aristaless-related homeobox gene (ARX), a transcription factor with a putative role in cortical development, was found to be associated with infantile spasm syndrome, X-linked lissencephaly with abnormal genitalia (XLAG) and other developmental abnormalities (Kitamura *et al.*, 1997; Miura *et al.*, 1997; Bienvenu *et al.*, 2002; Kato *et al.*, 2004; Cobos *et al.*, 2005, 2006). The identification of a genetic cause of isolated infantile spasm syndrome provides a possible inroad, through understanding the consequence of ARX loss in the CNS, to defining the underlying pathogenesis of infantile spasm syndrome and other developmental epilepsies.

Arx is expressed in the developing hypothalamus, thalamus, basal ganglia and cerebral cortex beginning at embryonic Day 8 (E8) and persisting through early postnatal life (Kitamura *et al.*, 1997; Miura *et al.*, 1997; Bienvenu *et al.*, 2002; Cobos *et al.*, 2005, 2006). Although the functions of *Arx* have not been fully elucidated, it appears to play important roles in pallial progenitor cell proliferation, non-radial cell migration of interneurons from the sub-pallial ganglionic eminence into the developing cortex, regulation of radial migration and basal ganglia development (Kitamura *et al.*, 2002; Colombo *et al.*, 2007; Friocourt *et al.*, 2008). Male mice carrying an engineered mutation in *Arx* recapitulate many

aspects of the human condition (XLAG) with abnormal appearing basal ganglia, an anomalous corpus callosum, cortical layer abnormalities and most notably, a profound deficit in interneuron migration (Kitamura *et al.*, 2002; Collombat *et al.*, 2003). Unfortunately, the mice are perinatal lethal, limiting postnatal physiological and behavioural analyses. The finding of major changes in interneuron migration in mice, caused by mutations in the same gene that is causally linked to patients with infantile spasm syndrome, implicates interneuron dysfunction as the underlying pathogenesis for genetic developmental disorders.

Recently Dobyns and colleagues hypothesized that loss of (inhibitory) interneurons (not excitatory projection neurons) in the cortex is an important factor in development of the particularly intractable character of seizures in some patients with malformations of cortical development (Kato and Dobyns, 2005). Specifically, these authors hypothesized that the epilepsy phenotype observed in children with *ARX* mutations results primarily from a deficit in forebrain cerebral cortical interneuron function that they designated an 'interneuronopathy' (Kato and Dobyns, 2005). To directly test this hypothesis and further investigate the mechanism by which *Arx* mutations cause functional neurologic disorders, we generated a mouse line carrying a floxed allele for Arx (Arx^{fl}) and crossed them to $Dlx5/6^{CIG}$ mice to target genetic ablation of Arx to subpallial derived neurons in which Dlx5/6 is selectively expressed. Both male and female mutant mice demonstrated early childhood onset 'developmental' epilepsy resembling that observed in patients with *ARX* mutations. By selectively deleting *Arx* from interneurons and obtaining this phenotype, our data provide direct functional support for the interneuronopathy hypothesis. To further support these data, we present the clinical phenotype of epilepsy and mental retardation in human females heterozygous for severe mutations in *ARX*, and show that the female mutant mouse model recapitulates the human female heterozygous state.

Methods

Animal studies

The Children's Hospital of Philadelphia animal care and use committee approved all animal experiments. The animals were kept in standard

mouse cages, on a 12-h light/dark cycle, and allowed free access to food and water. Mice were generated with a floxed Arx allele by homologous recombination. Mice carrying the floxed Arx allele and genotyping of this mouse are described elsewhere (Fulp et al., 2008). $Arx^{fl/fl}$ and $Arx^{fl/+}$ females were then crossed to $Dlx5/6^{CIG}$(cre-IRES-GFP) males generously provided by Dr Kenneth Campbell (Stenman et al., 2003). $Arx^{fl/+ \text{ or } Y}$, $Dlx5/6^{CIG}$ and the CD1 and C57/Bl6 background genotypes were all considered controls, but reported separately for seizure occurrence and background abnormalities as we first needed to show that mice carrying the floxed allele or an insertion of the Dlx5/6-cre-IRES-GFP did not have an epilepsy or morphological phenotype. Once this was determined the Floxed, Cre and wild-type animals could be pooled into a 'control' group.

Genotype nomenclature

Throughout the paper, conditional knockout male mice with no normal copies of Arx in the ganglionic eminence are designated $Arx^{-/Y}$; $Dlx5/6^{CIG}$, heterozygous females with only one functional copy of Arx are $Arx^{-/+}$;$Dlx5/6^{CIG}$, control female and male mice with floxed but functional copies of Arx are $Arx^{fl/+}$ or $Arx^{fl/Y}$ and female or male mice carrying the insertion of cre-IRES-GFP are $Dlx5/6^{CIG}$.

EEG recordings

All mice recordings were performed using a Stellate-Harmonie (Stellate Inc., Montreal, Canada) 16-bit, 24 channel digital EEG machine, sampling at 200 Hz with a hard wired 100 Hz low pass anti-aliasing filter. For adult animals (>3 months postnatal age) unity gain pre-amplifiers were constructed in house from TI LM2478 quad operational amplifier integrated circuits (Texas Instruments). Cortical electrodes were constructed from #0 × 1/8″ self tap screws (Small Parts Inc.) and hippocampal (Hp) electrodes from mono-polar 0.005 in stainless steel wire (125 μm; A-M systems, Carlsborg, WA, USA). Electrodes were placed under inhaled isoflorane anesthesia, with pre-medication with ketamine/xylazine. For adult animals (>3 months postnatal age) electrodes were guided into the cortex (region M1 bilaterally) and hippocampus (CA1 layer bilaterally) using the following sterotaxic coordinates [from Bregma—cortical: 1.0 mm Anterior–Posterior (A–P) and 1.5 mm medial–lateral (M–L); HP: −2.2 mm A–P, 2.0 mm M–L and 1.2 mm ventral]. Once in the correct position, 0.005 in stainless steel wire was attached to the cortical screws and the all electrodes were held in a six pin Delran pedestal (Plastics One, Roanoke, VA, USA). Ground and reference electrodes were placed directly behind the Lambda suture on either side of the midline. For immature animals (P14–16; 1–2 days post eye opening), the electrodes were 0.005 in. stainless steel mono-polar electrodes placed into the cortex using the following stereotaxic coordinates: anterior and posterior cortical wires were 1.0 mm A–P, 1.2 mm M–L and −2.0 mm A–P and 1.5 mm M–L, respectively. As with the adult mice, the pedestal was held in place by dental cement. The immature animals were recorded in a blinded fashion, prior to knowing the genotype of any members of the litter. Following surgery, all animals were allowed to recover under a heat lamp or on a servo-controlled heating pad, until spontaneously mobile. The animals were then returned to their home cage for a minimum of 2 h and up to 6 h before being hooked up to the recording apparatus. The adult animals were recorded for a minimum of 24 h and as long as 30 days. Typically, the controls were recorded for 72–96 h and the $Arx^{-/y}$;$Dlx5/6^{CIG}$ male and $Arx^{-/+}$;$Dlx5/6^{CIG}$ female Hets for 96–120 h. The immature animals were recorded for 24 h and given gavage feeding prior to recording and re-gavaged and given IP saline after 12 h to ensure continued hydration and nutrition. The immature animals were sacrificed and processed for histological studies immediately after the recordings. The animals were allowed free access to water and food in the recording cages during the duration of the recordings.

EEG analysis

The EEG tracings were visually reviewed for the presence of electrographic seizures. If a seizure was suspected, the video was reviewed to ensure the electrographic change was associated with a behavioural seizure and not associated with movements such as scratching that could produce an artefact. When assessing for electrographic seizures we scanned for the presence of both rhythmic repetitive spike and sharp activity lasting ⩾5 s as well as for periods where a spike or higher voltage transient was followed by a few seconds of reduced EEG amplitude or paroxysmal background attenuation (i.e. resembling the electrodecrements associated with infantile spasms in humans). The latter were carefully reviewed, in slow motion and expanded time scale, to ensure that spasm-like movements occurred after the initial transient activity.

The EEG was also reviewed to characterize the background activity, including the amplitude, frequencies and the presence of normal transients (e.g. theta in HP electrodes during exploration), and sleep activity as well as interictal epilpetiform abnormalities such as spikes. These patterns were compared in all groups monitored. Quantitative assessment of background activity was performed by randomly selecting six 30-min segments from throughout the recording period. Fast Fourier transforms (using MATLAB 2006b 7.3 algorithm-Mathworks, Natick, MA, USA) and Root mean square voltage amplitudes were calculated for each segment. The selected EEG segments, individual animals, and genotypes were considered independent variables and compared by implementing a multi-way ANOVA in MATLAB computing environment (see Statistics section).

Gross anatomy and histology

After EEG recordings the animals were deeply anesthetized then sacrificed. The brains were harvested from the brainstem to the olfactory bulbs, and weighed. The brains were fixed in 4% paraformaldehyde overnight at 4°C then transferred to PBS. Each whole brain was carefully viewed to characterize gross morphologic differences. Four tissue blocks were prepared: (i) from the posterior boundary of the olfactory bulbs to 2 mm posterior on the frontal cortex; (ii) from the frontal cortex to 2 mm anterior to the optic chiasm; (iii) from 2 mm anterior to 1 mm posterior to the chiasm; and (iv) from 1 mm posterior to the chiasm to the occipital cortex. The four tissue blocks were embedded in paraffin and cut into 4 μm sections for histology and immunohistochemical studies. One slide per region was stained with haematoxylin and eosin. Immunohistochemistry was performed using a standard protocol with antibodies against interneuron markers (Calb-calbindin, Calb2-calretinin and Parv, parvalbumin), GFP (anti-GFP) and Arx (see Supplementary Table 1 for manufacture information and staining parameters) (McManus et al., 2004a, b). Antigen retrieval was performed by heating the slides in citric acid buffer for 5 min in a microwave (2 min on high, 3 min at medium power).

The tissue was visualized using a Lieca DMR microscope (Lieca Microsystems, Bannockburn, IL, USA) equipped with epiflorescence and light microscopy. The images were acquired on an Orca digital Camera (Hamamatsu, Hamamatsu City, Japan) and processed in Image Pro software for cell counting.

Cell counting

Sections from the most anterior block (in M1 and lateral neocortex), sections from the optic chiasm block (S1 and lateral neocortex), and sections through the hippocampus (in sagittal section) were chosen for cell counting. Two 10× magnification images were taken and stitched together to produce a continuous image from the ventricular to pial surface. Cells, fully labelled, were measured and numbered from a reference point on the ventricular surface in the middle of the acquired image. This method was performed as a way to measure distance from the ventricular surface (layer and location information) and well as number cells (total quantitative information). The images were blinded to the individual doing the counting. Counts between sections were averaged for each animal and then compared between genotypes using an ANOVA in MATLAB.

Human studies

The University of Chicago Institutional Review Board approved all human studies. Patients with ARX-related phenotypes and their unaffected relatives were ascertained from clinicians in North America and Europe. Clinical information and DNA samples were collected with informed consent. Mutation analysis was done using routine sequencing methods in a research lab with all positive results confirmed in the University of Chicago Genetic Services Laboratories. FISH was performed by standard methods as previously described (Christian *et al.*, 2008).

X-inactivation method

To analyse the X-inactivation pattern in heterozygous females, we examined the methylation status at the Androgen Receptor (AR) locus. Initially, 200 ng genomic DNA was digested in a 50 μl reaction volume with 40 U of HpaII in buffer # 1 (NEB) overnight at 37°C, following the published protocol (Plenge *et al.*, 1997). After digestion the enzyme was inactivated at 65°C for 30 min and 15 ng of undigested or digested DNA was used for amplification. For each PCR, a 10 μl master mix with 1 μl 10 × PCR Buffer I containing 15 mM MgCl$_2$ (ABI, Foster City, CA, USA), 0.2 μl 10 mM dNTP (ABI), 0.05 μl of 1000 U Ampli Taq Gold (ABI) enzyme, 0.8 μl of 10 μM forward and reverse primers (IDT, Coralville, IA, USA) and 7.95 μl of sterile H$_2$O (Sigma-Aldrich, St Louis, MO, USA) was added. The Primers are AR-F: 5'-TCCAGAATCTGTTCCAGAGCGTGC-3' and AR-R: 5'-GCTGTGAAG GTTGCTGTTCCTCAT-3'. The PCRs were run using the following conditions: hot start at 95°C for 3 min, 95°C for 1 min, 55°C for 1 min, 72°C for 1 min for 35 cycles followed by a final extension step at 72°C for 7 min. For genotyping analysis the forward primer was labeled with FAM on the 5'-end. Products were analysed on an ABI 3730 XL DNA sequencing analyser and processed using GeneMapper 3.7 software (ABI). The X-inactivation ratios were calculated as (d1/u1)/(d1/u1 + d2/u2), where d1 and d2 are the peak areas of smaller and larger alleles, respectively, from the digested sample and u1 and u2 are the corresponding alleles from the undigested sample (Kuo *et al.*, 2008). All the restriction digestion and amplification reactions were run in quadruplicate, and the average of four runs used for analysis. The coordinates of the amplicon are: chrX:66,681,781-66,682,068 in the UCSC Genome Browser, Human March 2006 build.

Statistical analysis

All statistics were performed in MATLAB using the statistics toolbox or Graph Pad software for the Fisher Exact test. A first test of differences between groups was performed using an N-way ANOVA. Each genotype was considered as an independent variable. For all ANOVA calculations the main effect had four degrees of freedom based on five genotypes: (i) wild-type (Bl6/C57); (ii) Arx$^{fl/+ \text{ or } y}$; (iii) Dlx5/6^{CIG}; (iv) Arx$^{-/+}$;Dlx5/6^{CIG} (female Hets); and (iv) Arx$^{-/y}$;Dlx5/6^{CIG} (CKO); and the level of significance was set at α = 0.01. As there was no difference between the control genotypes in either the EEG or cell count analysis (data not shown) the N-way ANOVA was repeated with the Arx$^{fl/+ \text{ or } y}$, Dlx5/6^{CIG} and WTs pooled as the control group and compared with the Arx$^{-/+}$;Dlx5/6^{CIG} (female Hets); and Arx$^{-/y}$;Dlx5/6^{CIG} (CKO males). In addition, the combined control group was independently compared with Student's *t*-tests to the Arx$^{-/+}$;Dlx5/6^{CIG} (female Hets) and Arx$^{-/y}$;Dlx5/6^{CIG} (CKO).

Results

Mouse studies

All studies were performed on crosses between female Arx$^{fl/+}$ or Arx$^{fl/fl}$ and male Dlx5/6^{CIG} mice. All expected genotypes were recovered from these litters, although not in complete Mendelian ratios due to fewer than expected Arx$^{-/y}$ males (data not shown). Once the mice were successfully generated and were found to live past the immediate postnatal period, experiments to elucidate the epilepsy phenotype were performed.

Adult EEG

To assess the mice for seizure activity, continuous video and intracranial EEG recordings (vEEG) were acquired in P90–P120 mice for up to 30 days. The background EEG was markedly disrupted in *Arx* mutant mice when compared to controls. Arx$^{-/Y}$;Dlx5/6^{CIG} mice (*n* = 3) were found to have a pattern of moderate to higher amplitude and faster frequency activity for the majority of the recording (Fig. 1C; upper and lower panels). The abnormal activity was more apparent in the Hp than the cortical (Cx) electrodes (Fig. 1C). Very frequent, and at times nearly continuous, sharp and spike-like waveforms (small arrows in Fig. 1C) were recorded in the Arx$^{-/Y}$;Dlx5/6^{CIG} mice. A major difference between the Arx$^{-/Y}$;Dlx5/6^{CIG} mice and controls was the clear lack of the normal 4–7 Hz rhythmic theta activity recorded when the animals were awake and exploring the cage. The Hp theta activity was rarely recorded, but when present had faster activity superimposed on the normal theta (Fig. 1C inset). Another difference was observed when the animals were sleeping. There was a general lack of the normal delta power and rhythmic delta activity seen in sleep (Fig. 2C). In contrast, Arx$^{+/Y}$, Arx$^{fl/Y}$ or Arx$^{fl/+}$, and Dlx5/6^{CIG} mice (*n* = 16, 8 and 7, respectively) all showed normal EEG background activity (Fig. 1A and data not shown) with rhythmic theta activity being recorded frequently when awake.

Unexpectedly, the EEGs of Arx$^{-/+}$;Dlx5/6^{CIG} female mice (*n* = 17) also exhibited abnormal background activity (Fig. 1B). The EEG patterns usually appeared normal, however, they were periodically interrupted by long runs of higher amplitude, faster rhythms and demonstrated excessive sharp activity (arrows in Fig. 1B, lower panel). This trait varied significantly between individual mutants; some Arx$^{-/+}$,Dlx5/6^{CIG} mice had essentially
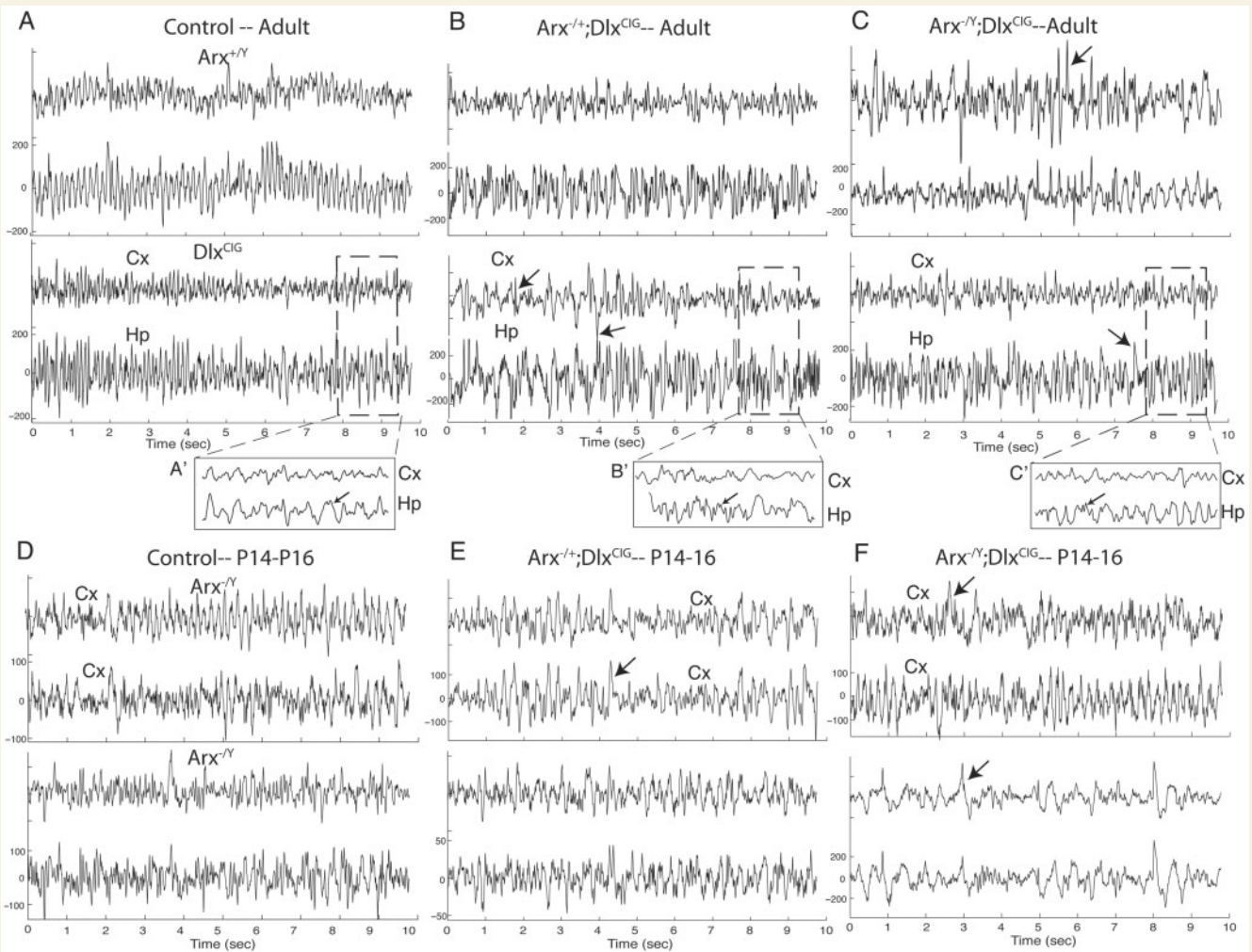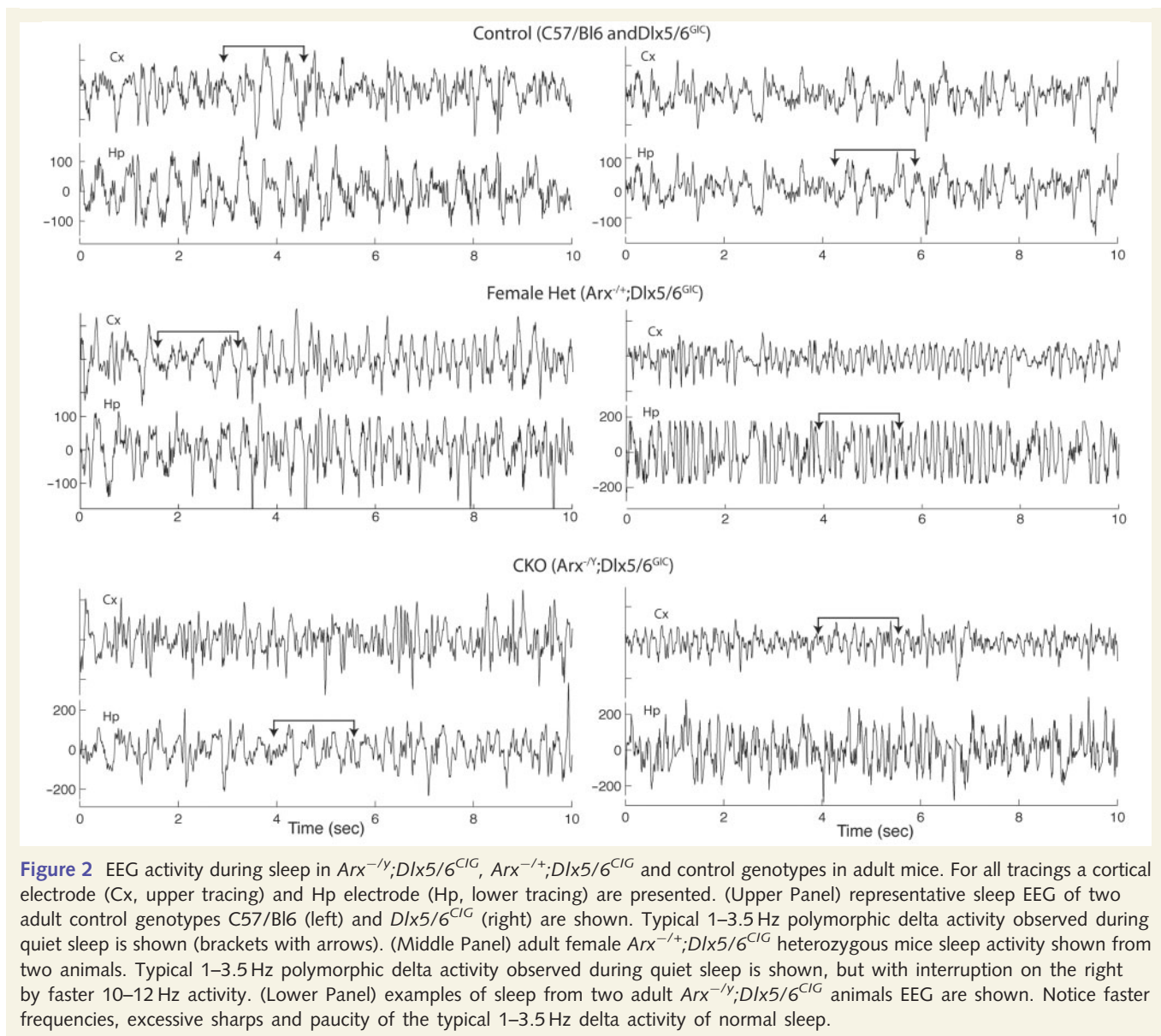
Figure 1 Background EEG findings of $Arx^{-/Y};Dlx5/6^{CIG}$, $Arx^{-/+};Dlx5/6^{CIG}$ and control genotypes in both adult and immature mice. For all tracings a cortical electrode (Cx; upper tracing) and Hp electrode (Hp; lower tracing) are presented. (**A**) Representative background EEG of two adult control genotypes $Arx^{fl/Y}$ (upper panel) and Dlx5/6^{CIG} (lower panel) are shown. Typical 5–7 Hz rhythmic activity observed during exploratory behaviors in wakefulness is observed. Expanded time scale of dashed box in the lower tracings is shown in A′. Arrow points to 5–7 Hz rhythm. Note lack of superimposed faster activity. (**B**) Adult female heterozygotes, $Arx^{-/+};Dlx5/6^{CIG}$, background activity is shown from two animals. Intermittent spike and sharp activity is present (arrows in lower traces). Inset (**B′**) shows faster time scale and increase in higher frequency activity. (**C**) Examples from two adult CKO $Arx^{-/Y};Dlx5/6^{CIG}$ animals are shown. Frequent spike and sharps are present and is nearly continuous in the upper tracing (arrows). Notice faster frequency and lack of rhythmicity of the resting background (see inset in C′). (**D–F**) Two representative background traces from controls (**D**), heterozygous females (**E**) and CKO (**F**) P14–16 immature animals are presented. The tracings from each of the animals are very similar in appearance. Intermittent higher voltage spikes were present in the $Arx^{-/Y};Dlx5/6^{CIG}$ Dlx5/6^{CIG} animals (**F**, lower tracing).

normal backgrounds whereas others exhibited more abnormal appearing patterns.

Background EEG findings were quantified by calculating root mean squared (RMS) energy and fast Fourier transforms (FFT) of five randomly chosen 30-min segments. This method prevents any bias in choosing the segments that are most different for quantification. Root mean squared measurements showed that the $Arx^{-/Y};Dlx5/6^{CIG}$ mice had higher amplitude recordings in the Hp electrodes, [ANOVA $P < 0.01$, Bonferroni *post hoc* confidence interval (CI) 4.299–68.098 CKO versus controls] but not in the cortical electrodes (Cx) (though it trended towards significance; ANOVA $P = 0.08$). There was no difference in amplitude

in either cortical or Hp electrodes between controls and the heterozygous females.

The calculated power spectrums were different between the $Arx^{-/Y};Dlx5/6^{CIG}$ and controls. Qualitatively, the FFT waveforms shifted to faster frequencies (Fig. 3) in the $Arx^{-/Y};Dlx5/6^{CIG}$ versus controls. These differences were tested by comparing the percentage of total energy within each of the typical EEG bandwidths (see Fig. 3 control). There were significant differences between the $Arx^{-/Y};Dlx5/6^{CIG}$ and controls with the $Arx^{-/Y};Dlx5/6^{CIG}$ mice having a decrease in delta activity ($P = 0.021$-Hp; 0.062-Cx) and an increase in faster frequency activity (Beta band $P < 0.01$-Hp and < 0.01-Cx and Gamma band $P < 0.01$ Hp and

Figure 2 EEG activity during sleep in $Arx^{-/Y};Dlx5/6^{CIG}$, $Arx^{-/+};Dlx5/6^{CIG}$ and control genotypes in adult mice. For all tracings a cortical electrode (Cx, upper tracing) and Hp electrode (Hp, lower tracing) are presented. (Upper Panel) representative sleep EEG of two adult control genotypes C57/Bl6 (left) and $Dlx5/6^{CIG}$ (right) are shown. Typical 1–3.5 Hz polymorphic delta activity observed during quiet sleep is shown (brackets with arrows). (Middle Panel) adult female $Arx^{-/+};Dlx5/6^{CIG}$ heterozygous mice sleep activity shown from two animals. Typical 1–3.5 Hz polymorphic delta activity observed during quiet sleep is shown, but with interruption on the right by faster 10–12 Hz activity. (Lower Panel) examples of sleep from two adult $Arx^{-/Y};Dlx5/6^{CIG}$ animals EEG are shown. Notice faster frequencies, excessive sharps and paucity of the typical 1–3.5 Hz delta activity of normal sleep.

$P = 0.097$ Cx) (Supplementary Table 2). The $Arx^{-/+};Dlx5/6^{CIG}$ female mice showed an intermediate phenotype with no decrease in Delta band activity ($P = 0.47$-Hp and $P = 0.62$-Cx) but an increase in faster frequency activity ($P = 0.01$-Hp, $P < 0.01$-Cx; and $P < 0.01$-Hp, $P < 0.01$-Cx beta and gamma, respectively) that is consistent with the variable background changes and the qualitative assessment that the more normal activity was interrupted by faster frequency activity.

In contrast to control mice, all adult $Arx^{-/Y};Dlx5/6^{CIG}$ mice developed spontaneous seizures ($n = 3$, Table 1). Two patterns of seizures were observed (Fig. $4A_{1-2}$ and A_3); an arrest of activity/freezing seizure (Fig. $4A_3$) and a whole body flexion or extension movement resembling epileptic spasms seen in infantile spasm syndrome (Fig. $4A_{1-2}$ and Supplementary Videos 1 and 2). Interestingly, 53% of $Arx^{-/+};Dlx5/6^{CIG}$ female mice also developed seizures ($n = 17$). The seizures in the $Arx^{-/+};Dlx5/6^{CIG}$ female mice consisted of convulsive Racine stage 5 seizures (Fig. $4B_1$, Racine, 1972), arrest

of activity or freezing seizures (Fig. $4B_2$; Supplementary Video 3 and 4), and epileptic spasm seizures (data not shown). No seizures were recorded in any $Arx^{fl/+}$, $Arx^{fl/Y}$ or $Dlx5/6^{CIG}$ mice ($n = 30$). All recorded seizures were brief (<5 min) and self-limited.

P14-16 mouse EEG

Having documented the seizure semiology in adults, we next determined if seizures were also present in developing mice, as developmental epilepsies typically begin during infancy and early childhood. We chose to record animals at P14–P17 as this is a period with approximately equivalent brain development to a 3- to 12-month-old infant (Rakic and Nowakowski, 1981; Avishai-Eliner *et al.*, 2002), a common time for the onset of infantile spasm syndrome. This time point also represented the earliest time intracranial electrodes could be reasonably implanted and secured to the pup cranium. Since P14–P17 is
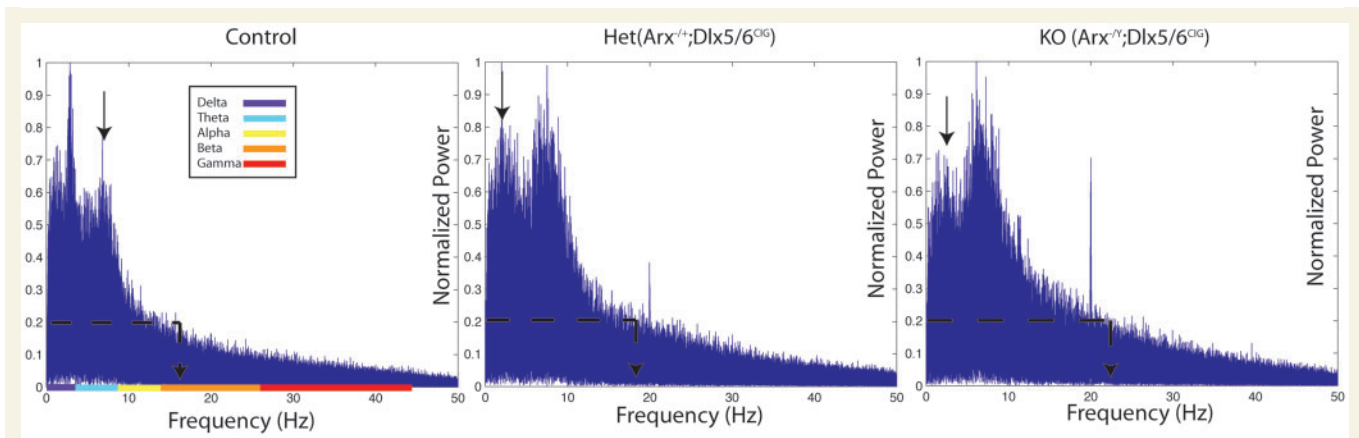
Figure 3 Fast Fourier Transformations from a random 30-min segment of each genotype show difference in background activity. Representative spectrums from Control (left- $Arx^{-/Y}$), $Arx^{-/+};Dlx5/6^{CIG}$-middle, and $Arx^{-/Y};Dlx5/6^{CIG}$-left are presented. x-axis = frequency; y-axis = normalized power. In control spectrum, the typical EEG frequency bandwidths are depicted in the left axis by colour. A shift from peak power in delta and theta bands in the controls to peak power in the higher frequency bands in the $Arx^{-/Y};Dlx5/6^{CIG}$-CKO is demonstrated by the arrows in each graph. The dotted line represents where two-third of total power falls and shifts from 17 Hz in $Arx^{fl/+}$ controls to 24 Hz in the CKO.

Table 1 Seizure occurrences in all genotypes in adult and immature mice

Mouse genotype	Seizures Present (%)			
	n	Adult	n	Immature
Wild-type	16	0	4	0
Arx-Flox	8	0	14	0
Dlx-cre	7	0	1	0
Het Female	17	53	7	57
KO male	3	100	3	100

Adult (left columns) and immature (right columns) mice of each genotype, the numbers of animals in each group (n) and the percentage with seizures (%) are listed.

pre-weaning, recordings were limited to 24 h and the animals were sacrificed after the recordings. The background was generally slower with lower voltage when compared with mature animals (Fig. 1D–F). When compared to age-matched controls, the background characteristics of the $Arx^{-/Y};Dlx5/6^{CIG}$ mice ($n = 3$) exhibited no reproducible differences (Fig. 1D–F). However, in one animal large amplitude spikes occurred infrequently throughout the recording of this $Arx^{-/Y};Dlx5/6^{CIG}$ mouse (Fig. 1F$_2$). In contrast to the adult mice, $Arx^{-/+};Dlx5/6^{CIG}$ female mice had similar background EEG activity to age-matched controls (Fig. 1E).

Similar to the adult animals, all P14-P17 $Arx^{-/Y};Dlx5/6^{CIG}$ mice demonstrated spontaneous seizures (Fig. 4C, Table 1) consisting of body arching with forelimb clonus and rearing (Racine Stage 5) (Supplementary Video 5). Female $Arx^{-/+};Dlx5/6^{CIG}$ mice also developed spontaneous seizures, at the same rate as their adult counterparts (57%, $n = 7$, Table 1). A single type (Racine stage 5) of seizure was recorded in the female pups. No epileptic spasm

seizures were recorded at this age. None of the immature control animals seized (Table 1, $n = 19$). Collectively, the video EEG0 recordings show that Arx mutant mice develop a single, non-spasm seizure type in early life that changes with maturation such that adult males develop seizures with features resembling human infantile spasm syndrome. These data indicate that loss of Arx results in developmental epilepsy that evolves over the life of the animals.

Interneuronal deficits

We next sought to define and correlate neuroanatomical defects with the presence of seizures. We found that independent of genotype the brains of immature P14–P17 and adult Arx mutants showed no specific anatomical defects (data not shown). This differed from the germline knockout mice reported by Kitamura et al. who found hypoplasia of the olfactory bulbs and corpus collosum (Kitamura et al., 2002). This difference is due to our model having only a knockout of Arx in interneurons. Similarly, no body or brain weight differences were found for the adults (Supplementary Fig. 1).

Although the postnatal $Arx^{-/Y};Dlx5/6^{CIG}$ and $Arx^{-/+};Dlx5/6^{CIG}$ mouse brains appeared grossly normal, we identified interneuron subtype specific defects. Immunohistochemistry was performed to assess cortical interneuron subpopulations in the brains of adult animals (Fig. 5A–C). Sections from the anterior M1 region, anterior ventral lateral neocortex, posterior S1 and ventral lateral neocortex, and hippocampus were analysed. Blinded counts from these four cortical regions were used to validate the subjective impression from the immunohistochemistry. The most prominent findings were a reduction of calbindin labeled neurons in the neocortex of both $Arx^{-/+};Dlx5/6^{CIG}$ and $Arx^{-/Y};Dlx5/6^{CIG}$ mice (Fig. 5A, and supplementary Fig. 2, ANOVA $P < 0.01$, $Arx^{-/+};Dlx5/6^{CIG}$ versus Controls CI 0.0658–0.2292, $Arx^{-/+};Dlx5/6^{CIG}$
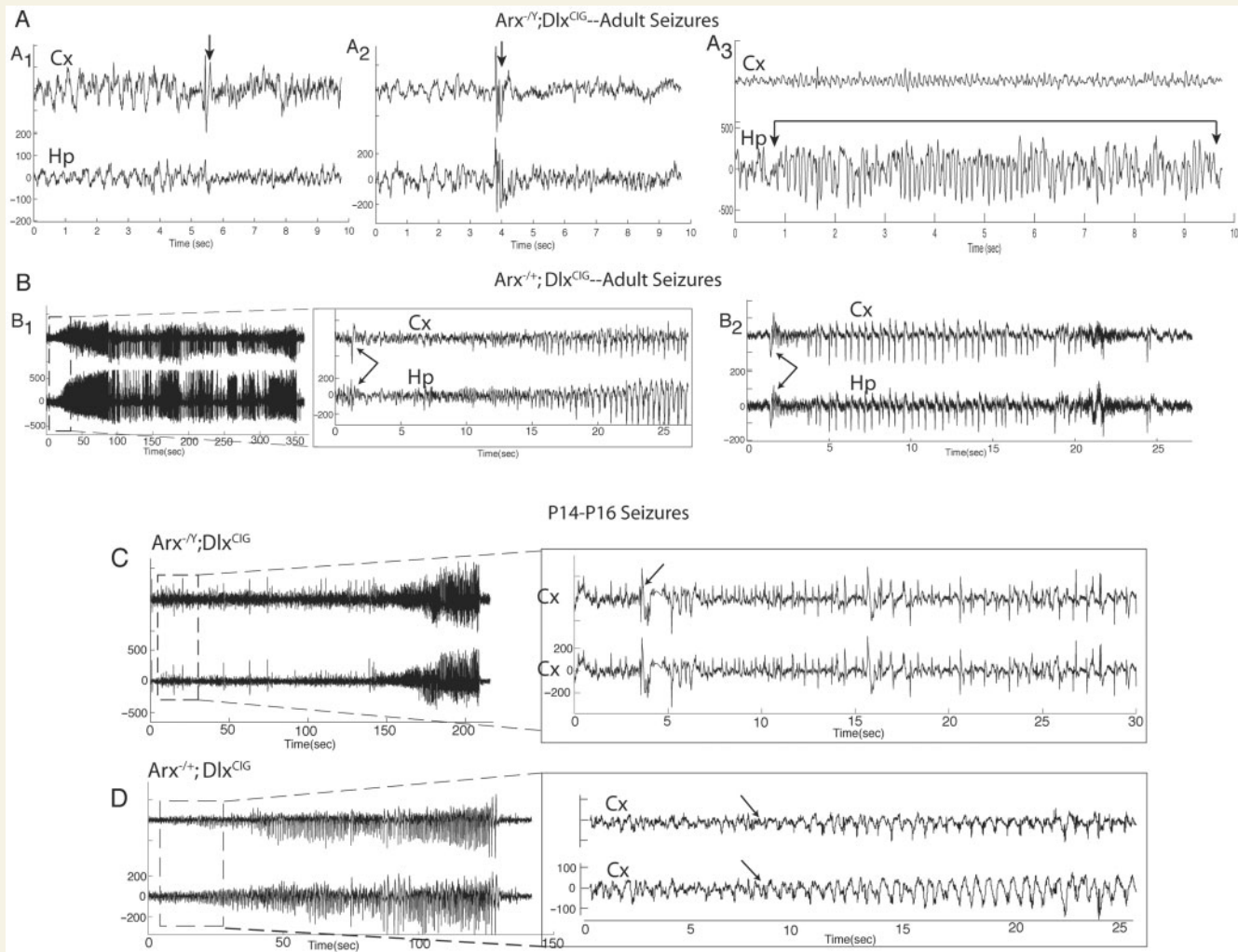
Figure 4 Examples of the electrographic changes during seizures in the $Arx^{-/+};Dlx5/6^{CIG}$ females and $Arx^{-/Y};Dlx5/6^{CIG}$ CKO males in adults and immature animals. (**A**) The two seizure types in the adult $Arx^{-/Y};Dlx5/6^{CIG}$ CKO males are presented. All CKO ($n=3$) had these seizure types. A_1 and A_2 are examples of seizures where the animal jerks forward after the higher voltage spike and slow wave activity (arrows), which is frequently followed by a flattening of the recording (electro-decrement). A_3 shows repetitive spiking that builds in frequency that occurs when the animals freeze during normal waking activity. (**B**) The two seizure types in the adult $Arx^{-/+};Dlx5/6^{CIG}$ heterozygous females are presented. Fifty-three per cent of females had seizures represented by these tracings. B_1 depicts a convulsive-stage 5 seizure, which begins (see dashed boxed area with faster time scale showing onset) with a high amplitude spike and slow wave followed by repetitive spike and slow waves that build in frequency and amplitude. A freezing, arrest of activity, type seizure's EEG change is presented in B_2. (**C** and **D**) Seizures in the immature $Arx^{-/Y};Dlx5/6^{CIG}$ CKO males (C) and $Arx^{-/+};Dlx5/6^{CIG}$ females are presented. At this age, the seizures in the two groups were identical with both groups having convulsive type seizures. EEG shows onsets in dashed boxes. Onsets of spike and slow waves are illustrated (arrows).

versus $Arx^{-/Y};Dlx5/6^{CIG}$ CI 0.032–0.2369). In the hippocampus the staining pattern changed from cell body to mostly staining processes (Fig. 5C). Smaller changes were observed in the numbers and distribution of calretinin labelled neurons between genotypes (Fig. 5B) with a significant decrease in $Arx^{-/+};Dlx5/6^{CIG}$ mice versus controls (ANOVA $P=0.035$; CI 0.065–0.2292) and a trend towards a difference between $Arx^{-/Y};Dlx5/6^{CIG}$ mice versus controls (ANOVA $P=0.035$; CI 0.032–0.2369). In contrast, there was no clear change in Parvalbumin staining in the cortex (Supplementary Fig. 2; ANOVA $P=0.397$). These finding indicate that Arx is necessary for interneuron subtype specific development in mice.

Human studies

Human female phenotypes

In humans, *ARX* mutations have been identified in a wide spectrum of developmental disorders (Sherr, 2003; Gecz *et al*., 2006). Prior to and during this study, several reports of affected human females heterozygous for severe mutations in ARX have appeared (Proud *et al*., 1992; Bonneau *et al*., 2002; Kato *et al*., 2004), with one report describing a late onset phenotype (Scheffer *et al*., 2002). These data prompted a more thorough review of heterozygous females from families with known *ARX* mutations.
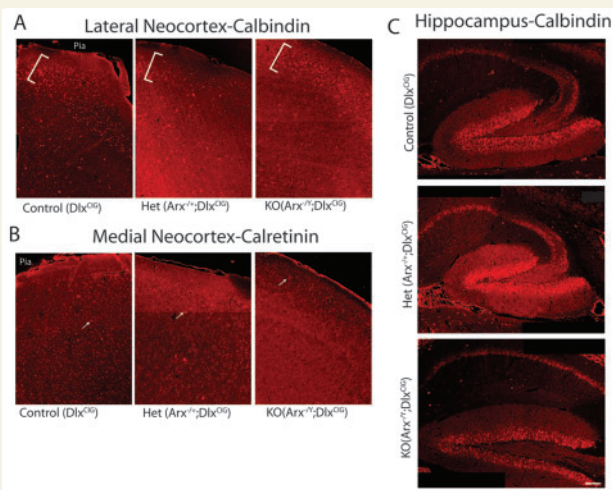
Figure 5 Representative Calbindin and Calretinin immuno-histochemistry in the neocortex and hippocampus of control, $Arx^{-/+};Dlx5/6^{CIG}$ and $Arx^{-/y};Dlx5/6^{CIG}$ animals. (**A**) Calbindin staining for control ($Dlx5/6^{CIG}$)-left, $Arx^{-/+};Dlx5/6^{CIG}$-middle and $Arx^{-/y};Dlx5/6^{CIG}$-right from the lateral neocortex frontal region is presented at 10× magnification. Layers two and three where the majority of calbindin interneurons are present and highlighted by the bracket. Calbindin interneurons are clearly reduced in the $Arx^{-/+};Dlx5/6^{CIG}$ compared with controls. A smaller reduction of Calbindin interneurons is present in the $Arx^{-/y};Dlx5/6^{CIG}$ mice. (**B**) Calretinin staining from medial neocortex for control ($Dlx5/6^{CIG}$)-left, $Arx^{-/+};Dlx5/6^{CIG}$ -middle and $Arx^{-/y};Dlx5/6^{CIG}$-right are presented at 10× magnification. A more subtle change in calretinin interneurons is present (arrows highlight labelled cells). (**C**) Calbindin staining in the hippocampus for control ($Dlx5/6^{CIG}$)-upper, $Arx^{-/+};Dlx5/6^{CIG}$-middle and $Arx^{-/y};Dlx5/6^{CIG}$-lower panels are presented. Pia–pial surface of brain. Scale bar = 100 μ in Hp images.

We have identified 25 heterozygous females with severe *ARX* mutations from 16 families, including 14 ascertained as mothers of affected genotypic males, nine of their other female relatives and two female probands. The 14 mothers of affected females were all asymptomatic when evaluated. The phenotype and mutations in these 25 females are summarized in Table 2, and representative clinical reports of one mother of a male proband, one female maternal first cousin of a male proband and one female proband are presented in the supplementary data.

Overall, 32% (8/25) of heterozygous females had significant developmental abnormalities, but the likelihood of disease varied significantly based on the method of ascertainment. Indeed, if female probands and mothers of affected male probands are excluded, 67% of heterozygous females presented with neurological symptoms. Among the 14 mothers of male probands, all had normal development and cognitive skills (14/14), and only one (1/12) had a series of three seizures in adolescence as described in the supplementary clinical report. However, half of those with imaging studies (3/6) had agenesis of the corpus collosum (ACC; Supplementary Fig. 3). In contrast, most other female relatives of male probands had abnormal phenotypes such as mental retardation (4/9), learning and attention problems (2/9) including one girl also diagnosed with pervasive developmental disorder, seizures (4/8) and ACC on brain imaging (5/6). The median age of seizure onset was approximately 6 months (range 0 months to 5 years) and none had infantile spasm syndrome. Only 33% (3/9) had completely normal development. Both female probands presented with infantile spasm syndrome, moderate to profound mental retardation and abnormalities on MRI imaging (see Table 2 and Supplementary Fig. 3). Significant differences were found in comparing the frequency of mental retardation ($P \leqslant 0.01$; Fisher exact test, $n = 25$) and seizures ($P < 0.01$; $n = 23$) between the mothers and other female relatives. The presence of ACC was not significantly different ($P = 0.257$, $n = 14$), most likely due to small numbers.

We previously reported the affected males from 12 of these families, who all had either XLAG or Proud syndrome resulting from either protein truncation mutations or substitutions at highly conserved amino acids within the homeodomain (Kato *et al.*, 2004). We found four novel ARX mutations in the four new families, the first a missense mutation in exon 4 near the 3'-end of the homeodomain (c.1135C>A; p.R379S) that alters a highly conserved arginine residue in a boy with severe mental retardation and infantile spasms, and in three female relatives. The next two are a duplication of 103 base pairs that includes the 3'-region of intron 4 and 5'-region of exon 5 (IVS4-82_ex5 1469dup103; p.489fs) in a boy with XLAG and his mother, and a single nucleotide deletion in exon 5 (c.1465delG; p.A488fs) in a female proband (Wallerstein *et al.*, 2008), both of which are predicted to cause truncation of exon 5. The last is a paracentric inversion disrupting *ARX* (see Supplementary Text and Supplementary Fig. 4) in another female proband. These data show that mutations that disrupt one copy of ARX in females can have pathogenic consequences.
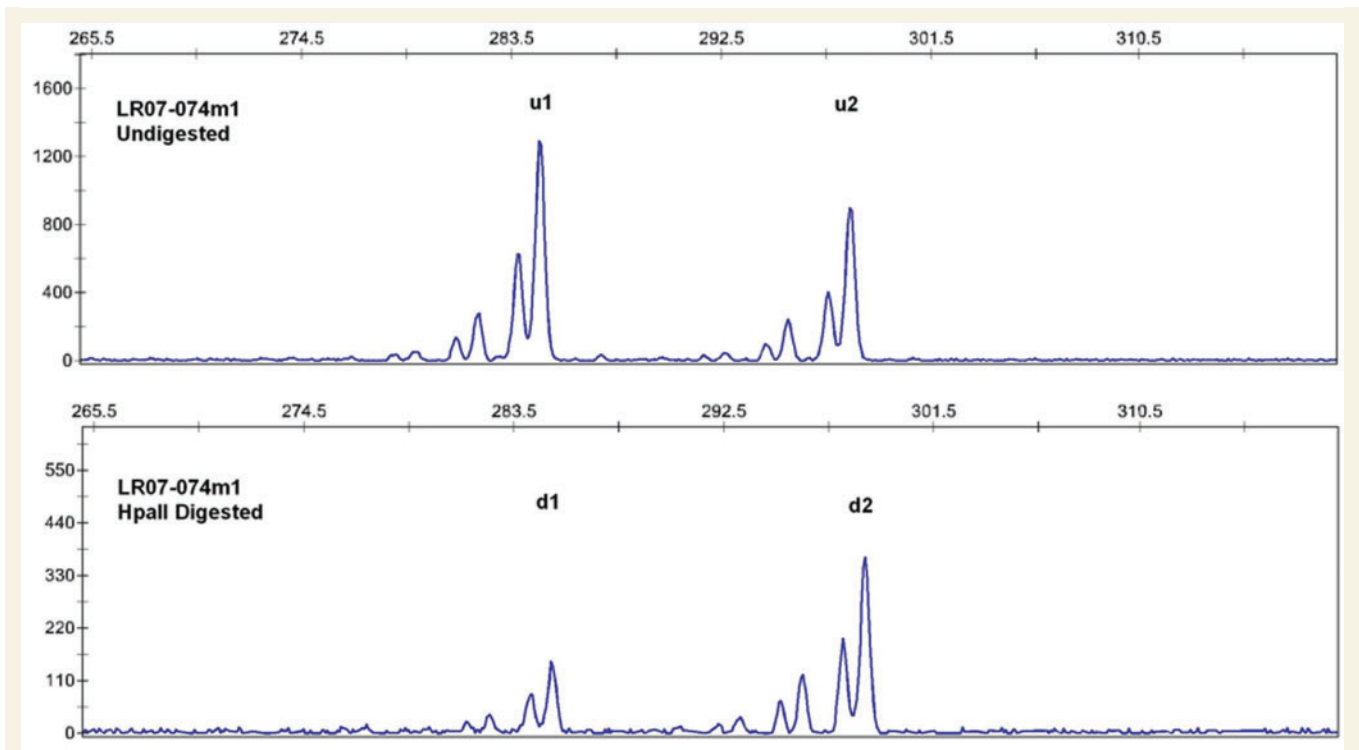
X inactivation

One possible explanation for finding distinct groups of symptomatic and asymptomatic heterozygous females involves differences in X chromosome inactivation (XCI) status. To test XCI status of these females, we performed DNA methylation studies of the human androgen receptor (*AR*) gene (Allen *et al.*, 1992). The human *AR* gene is commonly used in X-inactivation studies because the trinucleotide repeat in exon 1 is highly polymorphic. Our data (Fig. 6) show skewing of the XCI ratio of >80:20 in 4/18 (22%) females overall, which does not differ from the expected 14% (Amos-Landgraf *et al.*, 2006). Similarly, the XCI was not different between mothers and other female relatives, although this could be due to the small number of subjects available for study.

To further explore this question, we asked whether lesser differences in XCI status could explain differences in the phenotype between asymptomatic and symptomatic females. Note the opposite direction of XCI in two normal mothers (67 and 79 in LR01038m and LR07-074m1, Table 3) and their affected daughters (29 and 46 in LR01-038a2, and LR07-074a1, Table 3), and the same direction of XCI in a normal mother and her normal sister (05 and 21 in LR07-074m2 and LR07-074m1). These data support the hypothesis that subtle differences in XCI may explain why some females are symptomatic, but are not conclusive based

Table 2 Phenotype and genetic testing in heterozygous human females

Subject	Group	ARX mutation	Age	Development		Seizures			Brain imaging	Comments	References
				Status	Details	Y/N	Onset	Types			
LP94-058m	Mother	deleted	Adult	N		Y	12y	GTCS	...	See supplementary data	
LR00-023m	Mother	p.R332H	Adult	N		N			...		
LR00-052m	Mother	p.R332H	Adult	N		N			N		
LR00-175m	Mother	p.Q373X	Adult	N		N			N		
LR00-185m	Mother	p.G397fs	Adult	N		N			N	History of depression	
LR01-038m	Mother	p.G206fs	Adult	N		N			...		
LR01-330m	Mother	deleted	Adult	N		...			...		
LR02-083m	Mother	p.T333N	Adult	N		N			ACC-p		Proud, 1992
LR02-138m	Mother	p.E78X	Adult	N		N			ACC		Bonneau, 2002
LR02-139m	Mother	p.G66fs	Adult	N		N			...		Bonneau, 2002
LR02-195m	Mother	p.E78X	Adult	N		N			ACC		Bonneau, 2002
LR02-262m	Mother	p.L343Q	Adult	N		...			...		
LR04-427m	Mother	p.489fs	Adult	N		N			...		
LR07-074m1	Mother	p.R379S	39y	N		N			...		
LR01-038a2	Sister	p.G206fs	4y	MR	Moderate	Y	2 mo	...	ACC-p	hypotonia	
LR02-083r1	Cousin	p.T333N	Adult	MR	Mild	N			...	IQ 60, 44at 13, 17 years	Proud, 1992
LR02-083r6	Aunt	p.T333N	Adult	N		...	...	...	...		Proud, 1992
LR02-083r7	Aunt	p.T333N	31y	MR	Severe	Y	3 mo	...	ACC-p	Spasticity, scoliosis, contractures	Proud, 1992
LR02-138s1	Sister	p.E78X	6y	N		N			ACC-t	Walked 18 months, Duane anomaly	Bonneau, 2002
LR02-139s1	Sister	p.G66fs	5y	LD	Also ADD	N			ACC	ADD, poor balance, reported CVH	Bonneau, 2002
LR02-195a2	Aunt	p.E78X	27y	MR	Moderate	Y	1 y	GTCS	ACC-t	SZ meds stopped 11 years	Bonneau, 2002
LR07-074m2	Aunt	p.R379S	40y	N		N			...		
LR07-074a1	Cousin	p.R379S	10y	LD	Also PDD	Y	5y	Absence	N	See supplementary data	
LP94-090	Proband	inversion	2y	MR	Profound	ISS	In utero	ISS, mixed	ACC-t	See supplementary data	
LR06-362	Proband	p.A488fs	3y	MR	Moderate–severe	ISS	4 mo	ISS, mixed	Cysts	Atonic, myoclonic SZ, drooling, hypotonia	Wallerstein et al., 2008

All but one of the male probands in these families had XLAG and are reported in previous publications (Proud et al., 1992; Dobyns et al., 1999; Bonneau et al., 2002; Kato et al., 2004). We have incomplete data on final male proband, LR04-427, but the mutation is severe and the child's physician requested ARX testing.
Human patient data from females with ARX mutations. The relationship to a male patient (mother, aunt, sister, cousin) or if patient was the presenting family member (pro-proband), the ARX mutation (ARX column), developmental outcome (Dev column; MR- mental retardation, LD- learning disabilities, N- normal development), presence of seizures (Sz- column; Sz- seizure, ISS- infantile spasms, N- no seizures) and any brain abnormalities are presented. '...' represent that the data could not be obtained.
ACC = agenesis of the corpus callosum; ACC-p = partial ACC; ACC-t = total ACC; ADD = attention deficit disorder; CVH = cerebellar vermis hypoplasia; Cysts = basal ganglia cysts; ISS = infantile spasms; GTCS = generalized tonic–clonic seizures; LD = learning disability; mo = months; MR = mental retardation; N = normal; PDD = Pervasive developmental disorder; SZ = seizure(s); y = years,

Figure 6 X inactivation assay at human androgen receptor done by genotyping the CAG repeat after digestion by the *HpaII* methylation-sensitive enzyme. In the figure, the x-axis shows the size of the alleles and the y-axis shows the peak areas. u1 and u2 are the smaller and the larger alleles respectively from undigested sample, as seen in the top panel and d1 and d2 are the corresponding alleles from digested sample, the bottom panel. In this case, the smaller allele is active (unmethylated digested) and the larger allele is inactive (methylated undigested). The X inactivation ratios after calculating the peak areas are 21:79 listing the smaller allele first.

Discussion

These data show that interneuron-specific loss of *Arx* in mice results in a developmental form of epilepsy with characteristics similar to the phenotypes observed in humans with *ARX* mutations. Importantly, the mouse model recapitulates both the human male and female conditions with all the males and approximately half of the females presenting with epilepsy. The finding that an interneuron specific loss of *ARX* recapitulates many key characteristics of the human condition, with *Arx* expression left intact in the developing neocortex, suggests a critical role for interneurons in the pathogenesis of epilepsy in these patients and strongly support the concept of an 'interneuronopathy' (Kato and Dobyns, 2005), as the cause of some forms of developmental epilepsies, specifically including infantile spasms. This study is not the only model to endorse the interneuronopathy concept. Recent work in the Scn1a heterozygous knockout mice shows the pathophysiological mechanism for the seizures in those animals is an interneuron specific loss of the channel resulting in an overall reduction in inhibition (Yu *et al*., 2006).

on the small number of subjects and the likelihood of confounding crossovers between the AR and ARX loci, which are separated by 41.9 Mb.

The discovery of epilepsy in about half of female mice with heterozygous loss of Arx in interneurons is novel, and strongly supports our observation of epilepsy in about half of heterozygous or 'carrier' human females, at least among human females with unbiased ascertainment. An even higher proportion of females—about two-thirds—have abnormal development. The first reports of human *ARX* mutations described asymptomatic mothers as healthy carrier of the mutations. Our larger dataset confirms these reports, which we now attribute to a bias of ascertainment. Specifically, we hypothesize that heterozygous mothers of affected male probands have a bias of ascertainment toward a normal phenotype, which fits well with their having lived to adulthood and demonstrated high reproductive fitness. We also hypothesize the corollary that female probands have a bias of ascertainment toward an abnormal phenotype. These data are also consistent with many other X-linked disorders in humans, in which a substantial and sometimes large proportion of heterozygous females are affected, although they are typically less severely affected than hemizygous males (Dobyns *et al*., 2004).

One potential explanation for the variability in the female phenotype in this X-linked condition is X-inactivation. We tested the XCI status of the females by performing DNA methylation studies of the human *AR* locus (Allen *et al*., 1992). There are two possible issues with these studies. First, a potential difference in X-inactivation between blood and brain exists due to mosaicism at the time X-inactivation is established (Novelli *et al*., 2003;

Table 3 X chromosome inactivation data for females with heterozygous severe *ARX* mutations, including 2 probands, 11 mothers of probands and 5 other female relatives

LP#	Relation	Average
LP94-090	Proband	40:56
LR06-362	Proband	77:23
LR01-038m	Mother	**67**:33
LR01-038a2	Other	**29**:71
LR02-138m	Mother	95:05
LR02-138a2	Other	26:74
LR02-195m	Mother	**59**:41
LR02-195a2	Other	**83**:17
LR07-074m2	Mother	**05**:95
LR07-074m1	Other	*21*:79
LR07-074a1	Other	*54*:46
LP94-058m	Mother	61:39
LR00-023m	Mother	33:67
LR00-185m	Mother	79:21
LR01-331m	Mother	62:38
LR02-139m	Mother	11:89
LR04-427m	Mother	30:70
LR08-014m	Mother	54:46

Patient number, relation to proband, and averaged X-inactivation ratios are listed.

In this table, the X inactivation is shown as a ratio of the smaller:larger allele. The numbers in BOLD represent the shared allele between the mother of the proband and another female heterozygote (sister or maternal aunt of the proband) and the numbers in ITALICS, in family LR07-074, represent the shared allele between the two other female heterozygotes (maternal aunt and cousin). The shared allele could not be determined in family LR02-138.

Young and Zoghbi, 2004), although at least one study in Rett syndrome has suggested that the XCI pattern in blood is an accurate indicator of XCI patterns in the brain in a majority of patients (Shahbazian *et al.*, 2002). The other potential confounding issue with our X-inactivation studies, particularly the comparison of skewing within families is the possibility of crossovers between the ARX and AR loci. This data needs to be confirmed with either an XCI assay located close to the ARX gene or testing of polymorphic markers between the two genes. With these potential limitations, our data does not show clear evidence for increased skewing of XCI in either symptomatic or asymptomatic females, but the number of females tested is too low to draw firm conclusions. We found some differences in direction of XCI among female relatives in some families, but cannot yet conclude whether these differences are enough to impact the phenotype. We will need to study larger numbers of heterozygous females and test XCI status of the ARX gene itself in both humans and mouse, which will require development of new XCI assays in both groups, to settle the questions we raise here.

The epilepsy phenotype in the mice resembles an infantile spasms type seizure in several important ways. As in humans, the immature mice develop partial seizures (Racine Stage 5 partial seizures with secondary generalization) early in life that evolve into different seizure types, including an epileptic spasm seizure associated with an electrodecrement of EEG, and persist into adulthood. We recognize that evolution of the seizure phenotype in these animals differs from the human condition and appears to be 'reversed' with the epileptic spasms occurring earlier in humans and later in mouse. However, tonic or tonic–clonic focal seizures often precede or occur concurrently with the onset of infantile spasms in children (Carrazana *et al.*, 1993; Ohtahara and Yamatogi, 2001). Therefore, the apparent 'reversal' of the seizure phenotype that we observe may simply represent occurrence of the same early phenotype that is often observed in humans, rather than a reversal. Whether the sequence of seizures is 'reversed' or not, we do not believe that the minor discrepancies observed between human and mouse invalidate the Arx conditional knockout mouse as a viable model for the developmental epilepsies. The mouse and human central nervous systems differ significantly in development, structure and function, which could result in the persistence of a more immature cortical network. This in turn could explain any differences in evolution of the seizure phenotype.

Does this new *Arx* conditional mutant mouse serve as an animal model of infantile spasm syndrome? Specific criteria for animal models of infantile spasm syndrome have been proposed (Stafstrom and Holmes, 2002; Baram, 2007), and this model meets most of these criteria, importantly including an appropriate age parallel. Several other animal models of infantile spasm syndrome have been proposed in the past (Baram and Schultz, 1995; Velisek *et al.*, 2007), but each lacks more than one feature of a valid animal model of infantile spasm syndrome, particularly the age parallel and spontaneity of seizures. Our model has the added strength of recapitulating one of the known genetic causes of human infantile spasm syndrome. Overall, the *Arx* conditional knockout mouse will prove to be a useful model to study the underlying pathogenesis of infantile spasm syndrome and related early epileptic encephalopathies, as affected animals develop spontaneous seizures at the appropriate age including 'spasm-like' seizures, the seizures evolve as the animal matures, and the mice recapitulate the carrier state found in humans.

The proposed pathophysiological mechanism of the observed phenotype in these animals is a specific loss of interneurons resulting in an overall increase in excitation. Towards this end, a subtype specific loss of interneurons was found in this model, consisting of a primary loss of calbindin expressing interneurons. This subtype specific loss was not unexpected due to the use of this particular $Dlx5/6^{CIG}$ line as the Cre. This $Dlx5/6^{CIG}$ line employs the Dlx5/6 enhancer element I56i that has been shown to be more strongly expressed in Calbindin positive neurons compared to Calretinin positive cells (Ghanem *et al.*, 2007; Potter *et al.*, 2008). The Calretinin positive cells are under the control of a different enhancer element, URE2. The data from these studies suggest that 85–95% of Calbindin interneurons co-express with the I56i element but only 75–85% co-express with Calretinin (Ghanem *et al.*, 2007; Potter *et al.*, 2008). This difference likely explains the greater loss of Calbindin than Calretinin interneurons in our study. A second possible explanation for the seizure phenotype would involve pan-interneuronal abnormalities in these mice, but with the exception of the Calbindin subclass, the phenotype is not one of cell loss. Instead an abnormal

network, mis-specification or subtle alterations in location could account for the observed functional defect.

Another issue with the interneuron changes found in these studies are that $Arx^{-/+};Dlx5/6^{CIG}$ females have greater cell loss than the $Arx^{-/Y};Dlx5/6^{CIG}$ males. We found increased Calbindin cell loss in the $Arx^{-/+};Dlx5/6^{CIG}$ females, while Calbindin cell loss was more variable in males; one had an equivalent loss and the others less. This is an interesting and unexpected finding. One possible explanation is variability of the Cre-recombinase activity. This could be addressed *in vitro* but would not directly answer the question. Future work will address this interesting finding.

In summary, the epilepsy phenotypes in the $Arx^{-/Y};Dlx5/6^{CIG}$ male and corresponding female mice provide a new genetic mouse model of a human genetic developmental epilepsy, with many features of infantile spasms, and provides a useful model to study the underlying pathophysiology in this condition. Our results also significantly change the counselling regarding female fetuses or children with severe mutations of *ARX*. Further studies in these mice will permit a better understanding of the multiple roles of interneurons in establishing normal network properties in the developing brain. Understanding the pathophysiologic mechanism as to how these mice develop an infantile spasms-like phenotype may facilitate the development of more specific therapies against this malignant developmental epilepsy.

Supplementary material

Supplementary material is available at *Brain* online.

Acknowledgements

Funding

References

Allen RC, Zoghbi HY, Moseley AB, Rosenblatt HM, Belmont JW. Methylation of HpaII and HhaI sites near the polymorphic CAG repeat in the human androgen-receptor gene correlates with X chromosome inactivation. Am J Hum Genet 1992; 51: 1229–39.

Amos-Landgraf JM, Cottle A, Plenge RM, Friez M, Schwartz CE, Longshore J, et al. X chromosome-inactivation patterns of 1,005 phenotypically unaffected females. Am J Hum Genet 2006; 79: 493–9.

Avishai-Eliner S, Brunson KL, Sandman CA, Baram TZ. Stressed-out, or in (utero)? Trends Neurosci 2002; 25: 518–24.

Baram TZ. Models for infantile spasms: an arduous journey to the Holy Grail. Ann Neurol 2007; 61: 89–91.

Baram TZ, Schultz L. ACTH does not control neonatal seizures induced by administration of exogenous corticotropin-releasing hormone. Epilepsia 1995; 36: 174–8.

Bienvenu T, Poirier K, Friocourt G, Bahi N, Beaumont D, Fauchereau F, et al. ARX, a novel Prd-class-homeobox gene highly expressed in the telencephalon, is mutated in X-linked mental retardation. Hum Mol Genet 2002; 11: 981–91.

Bonneau D, Toutain A, Laquerriere A, Marret S, Saugier-Veber P, Barthez MA, et al. X-linked lissencephaly with absent corpus callosum and ambiguous genitalia (XLAG): clinical, magnetic resonance imaging, and neuropathological findings. Ann Neurol 2002; 51: 340–9.

Brunson KL, Eghbal-Ahmadi M, Baram TZ. How do the many etiologies of West syndrome lead to excitability and seizures? The corticotropin releasing hormone excess hypothesis. Brain Dev 2001; 23: 533–8.

Carrazana EJ, Lombroso CT, Mikati M, Helmers S, Holmes GL. Facilitation of infantile spasms by partial seizures. Epilepsia 1993; 34: 97–109.

Christian SL, Brune CW, Sudi J, Kumar RA, Liu S, Karamohamed S, et al. Novel submicroscopic chromosomal abnormalities detected in autism spectrum disorder. Biol Psychiatry 2008; 63: 1111–7.

Cobos I, Broccoli V, Rubenstein JL. The vertebrate ortholog of Aristaless is regulated by Dlx genes in the developing forebrain. J Comp Neurol 2005; 483: 292–303.

Cobos I, Long JE, Thwin MT, Rubenstein JL. Cellular patterns of transcription factor expression in developing cortical interneurons. Cereb Cortex 2006; 16 (Suppl 1): i82–8.

Collombat P, Mansouri A, Hecksher-Sorensen J, Serup P, Krull J, Gradwohl G, et al. Opposing actions of Arx and Pax4 in endocrine pancreas development. Genes Dev 2003; 17: 2591–603.

Colombo E, Collombat P, Colasante G, Bianchi M, Long J, Mansouri A, et al. Inactivation of Arx, the murine ortholog of the X-linked lissencephaly with ambiguous genitalia gene, leads to severe disorganization of the ventral telencephalon with impaired neuronal migration and differentiation. J Neurosci 2007; 27: 4786–98.

Friocourt G, Kanatani S, Tabata H, Yozu M, Takahashi T, Antypa M, et al. Cell-autonomous roles of ARX in cell proliferation and neuronal migration during corticogenesis. J Neurosci 2008; 28: 5794–805.

Frost JD Jr., Hrachovy RA. Pathogenesis of infantile spasms: a model based on developmental desynchronization. J Clin Neurophysiol 2005; 22: 25–36.

Fulp CT, Cho G, Marsh ED, Nasrallah IM, Labowski PA, Golden JA. Identification of Arx transcriptional targets in the developing basal forebrain. Hum Mol Genet 2008; 17: 3740–60.

Gecz J, Cloosterman D, Partington M. ARX: a gene for all seasons. Curr Opin Genet Dev 2006; 16: 308–16.

Ghanem N, Yu M, Long J, Hatch G, Rubenstein JL, Ekker M. Distinct cis-regulatory elements from the Dlx1/Dlx2 locus mark different progenitor cell populations in the ganglionic eminences and different subtypes of adult cortical interneurons. J Neurosci 2007; 27: 5012–22.

Kato M, Das S, Petras K, Kitamura K, Morohashi K, Abuelo DN, et al. Mutations of ARX are associated with striking pleiotropy and consistent genotype-phenotype correlation. Hum Mutat 2004; 23: 147–59.

Kato M, Dobyns WB. X-linked lissencephaly with abnormal genitalia as a tangential migration disorder causing intractable epilepsy: proposal for a new term, ''interneuronopathy''. J Child Neurol 2005; 20: 392–7.

Kitamura K, Miura H, Yanazawa M, Miyashita T, Kato K. Expression patterns of Brx1 (Rieg gene), Sonic hedgehog, Nkx2.2, Dlx1 and Arx during zona limitans intrathalamica and embryonic ventral lateral geniculate nuclear formation. Mech Dev 1997; 67: 83–96.

Kitamura K, Yanazawa M, Sugiyama N, Miura H, Iizuka-Kogo A, Kusaka M, et al. Mutation of ARX causes abnormal development of forebrain and testes in mice and X-linked lissencephaly with abnormal genitalia in humans. Nat Genet 2002; 32: 359–69.

Kuo PL, Huang SC, Chang LW, Lin CH, Tsai WH, Teng YN. Association of extremely skewed X-chromosome inactivation with Taiwanese women presenting with recurrent pregnancy loss. J Formos Med Assoc 2008; 107: 340–3.

McManus MF, Nasrallah IM, Gopal PP, Baek WS, Golden JA. Axon mediated interneuron migration. J Neuropathol Exp Neurol 2004a; 63: 932–41.

McManus MF, Nasrallah IM, Pancoast MM, Wynshaw-Boris A, Golden JA. Lis1 is necessary for normal non-radial migration of inhibitory interneurons. Am J Pathol 2004b; 165: 775–84.

Miura H, Yanazawa M, Kato K, Kitamura K. Expression of a novel aristaless related homeobox gene 'Arx' in the vertebrate telencephalon, diencephalon and floor plate. Mech Dev 1997; 65: 99–109.

Novelli M, Cossu A, Oukrif D, Quaglia A, Lakhani S, Poulsom R, et al. X-inactivation patch size in human female tissue confounds the assessment of tumor clonality. Proc Natl Acad Sci USA 2003; 100: 3311–4.

Ohtahara S, Yamatogi Y. Severe Encephalopathic Epilepsy in Infants: West Syndrome. In: Pellock JM, Dodson WE, Bourgeois BF, editors. Pediatric epilepsy: diagnosis and therapy. New York City: Demos; 2001. p. 177–85.

Plenge RM, Hendrich BD, Schwartz C, Arena JF, Naumova A, Sapienza C, et al. A promoter mutation in the XIST gene in two unrelated families with skewed X-chromosome inactivation. Nat Genet 1997; 17: 353–6.

Potter GB, Petryniak MA, Shevchenko E, McKinsey GL, Ekker M, Rubenstein JL. Generation of Cre-transgenic mice using Dlx1/Dlx2 enhancers and their characterization in GABAergic interneurons. Mol Cell Neurosci 2008; 40: 167–86.

Proud VK, Levine C, Carpenter NJ. New X-linked syndrome with seizures, acquired micrencephaly, and agenesis of the corpus callosum. Am J Med Genet 1992; 43: 458–66.

Racine RJ. Modification of seizure activity by electrical stimulation. II. Motor seizure. Electroencephalogr Clin Neurophysiol 1972; 32: 281–94.

Rakic P, Nowakowski RS. The time of origin of neurons in the hippocampal region of the rhesus monkey. J Comp Neurol 1981; 196: 99–128.

Scheffer IE, Wallace RH, Phillips FL, Hewson P, Reardon K, Parasivam G, et al. X-linked myoclonic epilepsy with spasticity and intellectual disability: mutation in the homeobox gene ARX. Neurology 2002; 59: 348–56.

Shahbazian MD, Sun Y, Zoghbi HY. Balanced X chromosome inactivation patterns in the Rett syndrome brain. Am J Med Genet 2002; 111: 164–8.

Sherr EH. The ARX story (epilepsy, mental retardation, autism, and cerebral malformations): one gene leads to many phenotypes. Curr Opin Pediatr 2003; 15: 567–71.

Stafstrom CE, Holmes GL. Infantile spasms: criteria for an animal model. Int Rev Neurobiol 2002; 49: 391–411.

Stenman JM, Wang B, Campbell K. Tlx controls proliferation and patterning of lateral telencephalic progenitor domains. J Neurosci 2003; 23: 10568–76.

Velisek L, Jehle K, Asche S, Veliskova J. Model of infantile spasms induced by N-methyl-D-aspartic acid in prenatally impaired brain. Ann Neurol 2007; 61: 109–19.

Young JI, Zoghbi HY. X-chromosome inactivation patterns are unbalanced and affect the phenotypic outcome in a mouse model of rett syndrome. Am J Hum Genet 2004; 74: 511–20.

Yu FH, Mantegazza M, Westenbroek RE, Robbins CA, Kalume F, Burton KA, et al. Reduced sodium current in GABAergic interneurons in a mouse model of severe myoclonic epilepsy in infancy. Nat Neurosci 2006; 9: 1142–9.

Zupanc ML. Infantile spasms. Expert Opin Pharmacother 2003; 4: 2039–48.